

TRIM28 is required by the mouse KRAB domain protein ZFP568 to control convergent extension and morphogenesis of extra-embryonic tissues

Maho Shibata¹, Kristin E. Blauvelt¹, Karel F. Liem, Jr² and María J. García-García^{1,*}

SUMMARY

TRIM28 is a transcriptional regulator that is essential for embryonic development and is implicated in a variety of human diseases. The roles of TRIM28 in distinct biological processes are thought to depend on its interaction with factors that determine its DNA target specificity. However, functional evidence linking TRIM28 to specific co-factors is scarce. *chatwo*, a hypomorphic allele of *Trim28*, causes embryonic lethality and defects in convergent extension and morphogenesis of extra-embryonic tissues. These phenotypes are remarkably similar to those of mutants in the Krüppel-associated box (KRAB) zinc finger protein ZFP568, providing strong genetic evidence that ZFP568 and TRIM28 control morphogenesis through a common molecular mechanism. We determined that *chatwo* mutations decrease TRIM28 protein stability and repressive activity, disrupting both ZFP568-dependent and ZFP568-independent roles of TRIM28. These results, together with the analysis of embryos bearing a conditional inactivation of *Trim28* in embryonic-derived tissues, revealed that TRIM28 is differentially required by ZFP568 and other factors during the early stages of mouse embryogenesis. In addition to uncovering novel roles of TRIM28 in convergent extension and morphogenesis of extra-embryonic tissues, our characterization of *chatwo* mutants demonstrates that KRAB domain proteins are essential to determine some of the biological functions of TRIM28.

KEY WORDS: KAP1, KRAB, Convergent extension, Extra-embryonic tissues, Gastrulation, Mouse

INTRODUCTION

Tripartite motif protein 28 (TRIM28), also known as KRAB-associated protein 1 (KAP1), KRAB interacting protein 1 (KRIP-1), or transcription intermediary factor 1 β (TIF1 β), encodes a TRIM/RBCC motif (RING finger, B box, coiled coil), plant homeodomain (PHD) finger and bromodomain protein that functions as a strong transcriptional repressor when bound to DNA (Friedman et al., 1996; Kim et al., 1996; Moosmann et al., 1996). The ability of TRIM28 to repress transcription has been proposed to reside in its ability to recruit chromatin-modifying enzymes, including the SETDB1 histone 3 lysine 9 methyltransferase (Schultz et al., 2002) and CHD3, a component of the nucleosome remodeling and histone deacetylation (NuRD) complex (Schultz et al., 2001). TRIM28 also binds heterochromatin protein 1 (Nielsen et al., 1999; Ryan et al., 1999), an interaction that affects TRIM28 localization to heterochromatic regions (Cammass et al., 2002), as well as some TRIM28 biological functions (Cammass et al., 2004; Herzog et al., 2010). In addition to its well documented roles as a transcriptional repressor, TRIM28 has recently been proposed to activate transcription through its ability to bind transcription factors, such as OCT3/4 (POU5F1 – Mouse Genome Informatics) (Seki et al., 2010), NGFI-B (NR4A1 – Mouse Genome Informatics) (Rambaud et al., 2009) and C/EBP β (CEBPB –

Mouse Genome Informatics) (Chang et al., 1998), raising the possibility that the formation of multimeric complexes with other proteins can modulate TRIM28 transcriptional activity.

Trim28 knockout mouse mutants fail to gastrulate and they die at embryonic day (E) 5.5 (Cammass et al., 2000). Additionally, TRIM28 has essential roles in a broad range of biological processes including spermatogenesis (Weber et al., 2002), silencing of endogenous retroviral elements (Rowe et al., 2010; Wolf et al., 2008a; Wolf and Goff, 2007; Wolf et al., 2008b), maintenance of embryonic stem (ES) cell pluripotency (Hu et al., 2009; Seki et al., 2010), epigenetic phenotypic variation (Whitelaw et al., 2010), cancer metastasis (Ho et al., 2009; Yokoe et al., 2009) and anxiety disorders (Alter and Hen, 2008; Jakobsson et al., 2008). Even though the transcriptional targets and co-factors of TRIM28 involved in the control of these biological processes are largely unknown, the DNA-binding specificity of TRIM28 is believed to be provided through its interaction with proteins of the Krüppel-associated box (KRAB) zinc finger protein family (Urrutia, 2003), a large family of transcription factors found exclusively in tetrapod vertebrates (Agata et al., 1999; Gebelein and Urrutia, 2001; Iyengar et al., 2011; Moosmann et al., 1996; Urrutia, 2003). Proteins of this family contain a KRAB domain, which mediates interaction with the TRIM28 N-terminal RBCC domain (Germain-Desprez et al., 2003; Peng et al., 2000; Peng et al., 2002) and a variable number of zinc finger motifs, which are thought to provide DNA-binding specificity to different targets (Emerson and Thomas, 2009; Gebelein and Urrutia, 2001). On the basis of its ability to enhance KRAB-mediated transcriptional repression, TRIM28 has been proposed to function as the universal co-repressor of all KRAB domain-containing proteins (Abrink et al., 2001; Agata et al., 1999; Friedman et al., 1996; Moosmann et al., 1996). Although KRAB domain zinc fingers represent the largest family of transcription

¹Department of Molecular Biology and Genetics, Cornell University, 526 Campus Road, Ithaca, NY 14853, USA. ²Sloan-Kettering Institute, Developmental Biology Program, 1275 York Avenue, New York, NY 10065, USA.

*Author for correspondence (garciamj@cornell.edu)

factors in mammals, comprising more than 300 genes (Emerson and Thomas, 2009; Huntley et al., 2006; Rowe et al., 2010), our current knowledge about the roles of individual KRAB domain proteins is limited to just a handful of these factors: ZFP568 is essential for embryo morphogenesis (Garcia-Garcia et al., 2008; Shibata and Garcia-Garcia, 2011), ZFP57 is required for the establishment and maintenance of genomic imprinting (Li et al., 2008), ZFP809 has been involved in silencing of retroviral elements in ES cells (Wolf and Goff, 2009), RSL1 and RSL2 regulate sex-specific gene expression in the liver (Krebs et al., 2003) and ZNF746 has been linked to *parkin*-dependent neurodegeneration (Shin et al., 2011). Even though several studies have demonstrated a functional link between some of these KRAB zinc finger proteins and TRIM28 (Gebelein and Urrutia, 2001; Li et al., 2008; Wolf and Goff, 2009), evidence supporting a role of TRIM28 as the universal co-repressor of all KRAB domain proteins is still limited. Furthermore, it is not yet clear whether TRIM28 is indispensable for the activity of individual KRAB domain proteins.

Our previous characterization of *Zfp568^{chato}* mutants identified roles for the KRAB zinc finger protein ZFP568 in the control of convergent extension and morphogenesis of extra-embryonic tissues (Garcia-Garcia et al., 2008; Shibata and Garcia-Garcia, 2011). *Zfp568* is widely and dynamically expressed during the early stages of mouse embryogenesis (Garcia-Garcia et al., 2008; Shibata and Garcia-Garcia, 2011). However, analysis of *Zfp568* chimeric embryos revealed that *Zfp568* is required in embryonic-derived cells to control morphogenesis of both embryonic and extra-embryonic tissues (Shibata and Garcia-Garcia, 2011). Here, we show that *chatwo*, an N-ethyl-N-nitrosourea (ENU)-induced mutation that causes a similar phenotype to *Zfp568* mutants, is a hypomorphic allele of *Trim28*. Our comparative analysis of *Trim28^{chatwo}* and *Zfp568^{chato}* mutant phenotypes provides strong evidence that ZFP568 and TRIM28 control morphogenesis of embryonic tissues through a common molecular mechanism. Consistent with this, we found that TRIM28 binds to ZFP568 and is required to mediate ZFP568 transcriptional repression. We found that *chatwo* mutations affect TRIM28 protein stability and repressive activity, disrupting both ZFP568-dependent and ZFP568-independent TRIM28 functions. Together with the analysis of null *Trim28^{KO}* mutants and embryos bearing a conditional inactivation of *Trim28* in embryonic-derived tissues, our results demonstrate that TRIM28 is indispensable for ZFP568 activity during embryo morphogenesis, and that TRIM28 is differentially required by ZFP568 and other factors in a tissue-specific manner. Our results uncover novel roles of TRIM28 during early mouse embryogenesis and provide mechanistic insight into the functions of TRIM28 as a co-factor of KRAB domain proteins.

MATERIALS AND METHODS

Mouse strains

chatwo was characterized on FvB/NJ and C57BL/6 *Mus musculus* strain backgrounds. Phenotype expressivity was quantified in embryos from congenic FvB/NJ and N7 backcrossed C57BL/6 animals. D7Mit178 and D7Mit76 polymorphic markers were used for genotyping. *Zfp568^{chato}* (Garcia-Garcia et al., 2008), *Trim28* knockout and *Trim28^{L2}* conditional mice (Cammass et al., 2000) were previously described. *Sox2Cre* mice were obtained from Jackson Laboratory (Hayashi et al., 2002). *Sox2Cre; Trim28^{L2/KO}* embryos were generated by crossing *Trim28^{L2}*, *Trim28^{L2/KO}* or *Trim28^{L2/+}* females to *Sox2Cre; Trim28^{KO/+}* males. Experiments with mice were carried out in accordance with institutional and national regulations.

Positional cloning of *chatwo*

The *chatwo* mutation was created on a C57BL/6/J genetic background, and outcrossed to FVB as described (Liem et al., 2009). Using a whole genome single nucleotide polymorphism (SNP) panel (Moran et al., 2006), the *chatwo* mutation was mapped to a 20 Mb region on proximal chromosome 7. Further mapping of meiotic recombinants narrowed the interval to SNPs rs31712695 and rs31644455. *Trim28* cDNA was sequenced as amplified (Superscript One-Step RT-PCR, Invitrogen) from wild-type and *chatwo* RNA extracted at E8.5 (RNA STAT-60, Tel-Test).

Embryo analysis

Embryos were dissected in 4% bovine serum albumin (BSA) in PBS. In situ hybridizations were conducted as previously described (Shibata and Garcia-Garcia, 2011). The *Trim28* probe was synthesized from a PCR-amplified cDNA fragment. Embryos were imaged in methanol, and cryosectioned at a thickness of 16 μ m. Immunohistochemistry was performed as described (Nagy, 2003) on 8 μ m cryosections. All comparisons of wild-type and mutant embryos are at the same magnification unless otherwise noted. Whole-mount embryos and sagittal sections are shown with anterior to the left and extra-embryonic tissues up. For western blotting, embryos were dissected in PBS and protein levels were quantified using Photoshop and linear regression analysis.

Expression of *Trim28* and intracisternal A-type particle (IAP) elements was tested by qRT-PCR on RNA samples extracted from independent pools of either wild-type, *Zfp568^{chato}*, *Trim28^{chatwo}* and/or *Trim28^{KO}* embryos collected at E7.5 or E8.5 (RNA STAT-60, Tel-Test). SYBR Green real-time PCR was used to quantify cDNA samples synthesized using Superscript III First-Strand Synthesis (Invitrogen). Expression of IAP elements was tested on DNaseI-treated (Roche) RNA samples. The absence of contaminating genomic DNA was confirmed by performing the assay in absence of reverse transcriptase.

Yeast two-hybrid assays

Gal4DBD and AD fusion plasmids were sequentially transformed into AH109 yeast strain using Matchmaker GAL4 Two-Hybrid System 3 (Clontech). Colonies were re-plated onto Ade-His-Leu-Trp- or Leu-Trp-X-alpha-gal plates.

Cell culture

HEK293, HEK293T or NIH3T3 cells were transfected with FUGENE 6 (Roche) or Lipofectamine 2000 (Invitrogen). A Leica DMI6000B fluorescent microscope was used for imaging. For immunoprecipitation, cells were lysed in buffer containing 150 mM NaCl, 50 mM Tris pH 7.5, 1 mM EDTA, 1% Triton X-100, 0.05% SDS and protease inhibitors. Immunoprecipitations were performed using 2-3 μ l of antibody and 25 μ l protein A/G agarose beads (Santa Cruz Biotechnology). For luciferase assays, HEK293T cells were transfected with pGL35XUAS firefly luciferase reporter, a Gal4DBD effector and pRL *Renilla* luciferase plasmids. Total amount of DNA transfected was held constant by co-transfecting pCMV-MYC as needed. Cells were assayed with the Dual-Luciferase Reporter System (Promega) 24 hours after transfection. For small interfering RNA (siRNA) knockdown, 8 pmol of *Trim28* siRNAs #1 (19779), #2 (19778) or non-silencing siRNA (Ambion) was transfected using Lipofectamine RNAiMax (Invitrogen). Cells were transfected with luciferase effectors and reporters 24 hours after siRNA transfection and luciferase was assayed after another 48 hours. For each luciferase assay, duplicate transfections and replicate lysates were measured for each condition ($n=4$). Firefly luciferase expression was normalized to *Renilla* to control for transfection efficiency. Percent luciferase expression was calculated compared with Gal4DBD. Lysates loaded for western blotting were normalized to *Renilla* expression. Statistical analysis was performed using paired, two-tailed *t*-test.

Reticulocyte translation assays

Translation was assayed using the TNT Coupled Reticulocyte Lysate and Transcend Non-Radioactive Translation Detection Systems (Promega) in the presence of 1 μ g plasmid DNA and 1 μ l of transcend tRNA (biotinylated lysine). Translated protein was visualized by western blotting using Streptavidin-HRP (1:10,000).

Antibodies

The following antibodies were used for western blotting, co-immunoprecipitation (co-IP) and/or immunofluorescence: anti-TRIM28 (4E6, Sigma-Aldrich; 1:500), anti-TRIM28 (H-300, Santa Cruz Biotechnology; 1:500), anti-TRIM28 (MA1-2023, Thermo Scientific; 1:25), anti-CHD3 (Abcam; 1:700), anti-SETDB1 (Millipore; 1:1000), anti-GAL4DBD (RK5C1, Santa Cruz Biotechnology; 1:500-1:800), anti-Myc (9e10, Hybridoma Bank; 1:250-1:1000), anti-Flag (M2, Sigma-Aldrich; 1:500-1:700), anti-HA (11, Covance 1:250), anti-HA (Y11, Santa Cruz Biotechnology; 1:500), anti-GAPDH (AB9482, Abcam; 1:8000), anti-mouse/rabbit HRP (Jackson ImmunoResearch; 1:10,000), anti-PECAM (eBioscience; 1:200), anti-rat Alexa 488 (Molecular Probes; 1:200), anti-mouse Alexa 568 (Molecular Probes; 1:200).

Constructs and primers

Plasmids pCDNA3.1-Gal4DBD-TRIM28, pCDNA3.1-Gal4DBD-TRIM28^{6KR}, pGL35XUAS firefly luciferase and pRL *Renilla* luciferase are described in Mascle et al. (Mascle et al., 2007). Other constructs were generated using primers as indicated in supplementary material Table S1.

RESULTS

chatwo causes embryonic and extra-embryonic defects similar to *Zfp568* mutants

chatwo mutants were isolated in an ENU mutagenesis screen for recessive mutations affecting development of the mid-gestation mouse embryo. Embryos homozygous for *chatwo* arrested prior to E9 with severe convergent extension defects and disrupted morphogenesis of extra-embryonic tissues (Fig. 1). *chatwo* mutants had a short anterior-posterior axis and failed to undergo gut closure, giving *chatwo* embryos a characteristic U-shape (Fig. 1A-D). Additionally, extra-embryonic tissues in *chatwo* mutants appeared constricted and the yolk sac developed numerous bubble-like protrusions (Fig. 1C,D, arrowheads). These phenotypes were remarkably similar to those of *chato* mutants, which are homozygous for a null allele of *Zfp568* (Fig. 1E,F) (Garcia-Garcia et al., 2008; Shibata and Garcia-Garcia, 2011), hence the name *chatwo* (*cha-two*; a second version of *chato*).

chatwo is a hypomorphic allele of *Trim28*

The *chatwo* mutation was mapped to a genetic interval on mouse chromosome 7 containing 9 genes (Fig. 2A). *Trim28* stood out amongst these candidates, given its previous involvement as a co-repressor of KRAB domain proteins (Abrink et al., 2001; Agata et al., 1999; Friedman et al., 1996; Moosmann et al., 1996), a large family of transcriptional regulators that includes ZFP568 (Emerson and Thomas, 2009; Huntley et al., 2006). Sequencing *Trim28* in *chatwo* mutants revealed two adjacent point mutations in the *Trim28* open reading frame (ORF), which respectively caused Cys713Trp and His714Asn non-conservative amino acid changes (Fig. 2B). These amino acid residues are highly conserved in human and *Xenopus* TRIM28, as well as in other members of the TIF1 protein family (Fig. 2D). The *chatwo* mutations in *Trim28* created a *Bs*I restriction site that was used to confirm linkage of these sequence changes to the *chatwo* phenotype (Fig. 2C).

Trim28-null embryos (*Trim28*^{KO}) arrest at ~E5.5, fail to gastrulate and lack expression of brachyury, a marker of the primitive streak (Fig. 2F) (Cammass et al., 2000; Wilkinson et al., 1990). We found that the *chatwo* allele had variable expressivity and sometimes caused developmental arrest at E7.5 (37.7%, *n*=182; supplementary material Fig. S1). However, the phenotype and stage of lethality of *Trim28*^{chatwo} mutants were always different to those of *Trim28*^{KO} embryos, as even *chatwo* embryos with an early developmental arrest expressed brachyury and were able to gastrulate (supplementary material Fig. S1C). These observations suggested that *Trim28*^{chatwo}

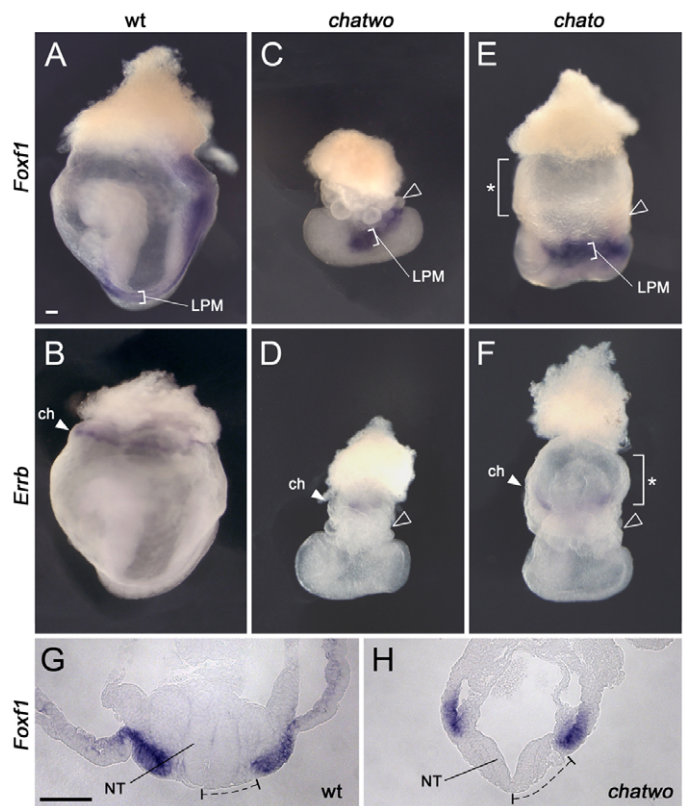


Fig. 1. Embryonic and extra-embryonic defects in *chatwo* and *Zfp568*^{chato} embryos. (A-F) Whole-mount in situ hybridizations with *Foxf1* (A,C,E) and *Errb* (B,D,F) probes on wild-type (A,B), *chatwo* (C,D) and *Zfp568*^{chato} (E,F) mouse embryos. Wild-type embryos are V-shaped, but *chatwo* and *Zfp568*^{chato} embryos display a characteristic U-shape. Open arrowheads in C-F point to the blistered yolk sacs. *Foxf1* expression (brackets in A,C,E) marks the lateral plate mesoderm (LPM). The bracket with an asterisk in E and F highlights the absence of blisters in distal yolk sac regions of *Zfp568*^{chato} embryos. Filled arrowheads in D-F point to *Errb* expression in the chorion (ch). (G,H) Transverse sections of embryos assayed for *Foxf1* expression. The dashed line highlights the distance between the embryonic midline and the LPM. NT, neural tube. Scale bars: 100 μ m.

could be a hypomorphic allele. To obtain genetic confirmation that *chatwo* disrupts *Trim28*, we analyzed *Trim28*^{chatwo/KO} embryos. Like *Trim28*^{chatwo} mutants, some *Trim28*^{chatwo/KO} embryos arrested at E7.5 (63.6%, *n*=7/11; Fig. 2H), whereas others survived until E8.5 (36.4%, *n*=4/11; Fig. 2G). Brachyury was expressed in all *Trim28*^{chatwo/KO} embryos examined, regardless of their stage of lethality, indicating that phenotypes of *Trim28*^{chatwo/KO} embryos are milder than those of *Trim28*^{KO/KO} mutants (Fig. 2E-H). These results support the hypothesis that *chatwo* mutations create a hypomorphic allele of *Trim28*. Additionally, the early lethality of *Trim28*^{KO} mice (Cammass et al., 2000) compared with that of *Trim28*^{chatwo} mutants and the null *Zfp568*^{chato} embryos suggests that TRIM28 is required during the early stages of mouse morphogenesis for processes other than those controlled by ZFP568.

chatwo affects ZFP568-dependent and ZFP568-independent roles of TRIM28

We showed previously that *Zfp568*^{chato} embryos have strong convergent extension defects, including failure to undergo anterior-posterior axis elongation, mediolateral expansion of mesenchymal

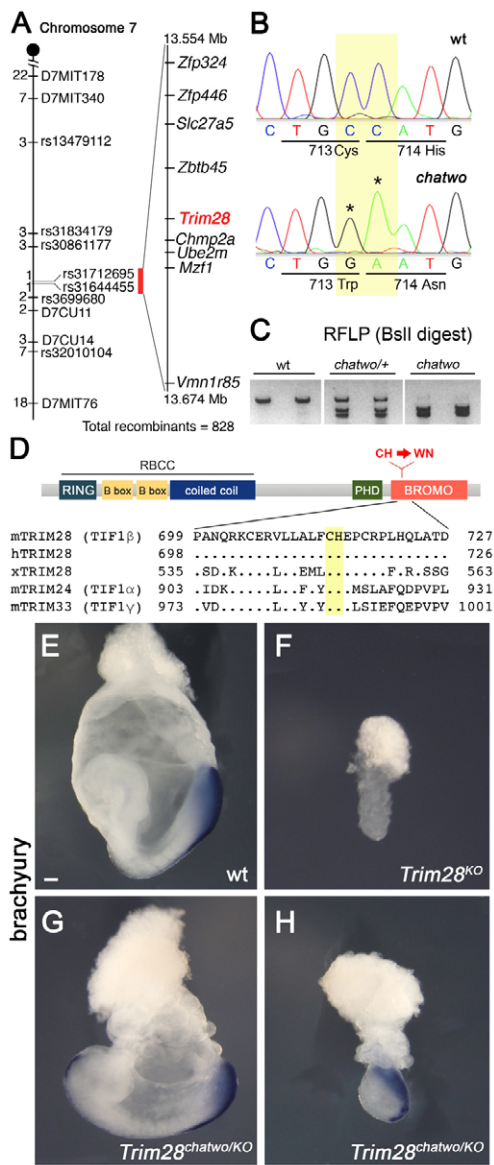


Fig. 2. *chatwo* disrupts *Trim28*. (A) *chatwo* was mapped to a 120 kb interval containing nine genes. The number of independent recombinants separating the mutation from the corresponding polymorphic markers on mouse chromosome 7 is indicated to the left. (B) Chromatograms showing *Trim28* cDNA sequence in wild type and *chatwo* mutants. Nucleotide positions 2142-2143 of *Trim28* ORF (yellow) were mutated in *chatwo* embryos (asterisks), producing C713W and H714N amino acid substitutions. Although ENU generally introduces single point mutations at random genomic locations (Anderson, 2000), an incidence of two mutations in the same gene has been previously found in ENU-induced mutants (K. V. Anderson, personal communication). (C) *chatwo* mutations create a *BsiI* restriction site. PCR-amplified wild-type DNA failed to digest with *BsiI*, but digestion was observed in fragments from heterozygote carriers (*chatwo/+*) and *chatwo* mutant embryos. These results were consistent in a collection of more than six heterozygote *chatwo* carriers and over ten mutant embryos. (D) Domain structure of TRIM28 showing location of *chatwo* mutations (red). Sequence alignments show the conservation of the CH residues mutated in *chatwo* (highlighted in yellow) in mouse, human and *Xenopus* TRIM28, as well as in other mouse TIF1 family members. (E-H) Whole-mount in situ hybridizations on wild-type (E), *Trim28*^{KO} (F) and *Trim28*^{chatwo/KO} (G,H) embryos using a probe for brachyury. Scale bar: 100 μm.

and epithelial tissues and an open neural tube (Garcia-Garcia et al., 2008). Phenotypic analysis confirmed that the phenotypes of *Zfp568*^{chato} mutants and *Trim28*^{chatwo} embryos with a late lethality were very similar. Analysis of *Foxf1* expression, which marks the lateral plate mesoderm (Mahlapuu et al., 2001), showed that this tissue was shorter and wider in late-lethality *Trim28*^{chatwo} mutants than in wild-type littermates (Fig. 1A,C, brackets), and was located further away from the midline (Fig. 1G,H, dashed line). Expression of *Meox1* (Candia et al., 1992) and *Twist* (Quertermous et al., 1994), showed that the somitic mesoderm was also mediolaterally expanded in late-lethality *Trim28*^{chatwo} embryos (not shown). Additionally, late-lethality *Trim28*^{chatwo} mutants failed to close the neural tube (Fig. 1G,H). Expression of transthyretin (*Ttr*) (Cereghini et al., 1992), which labels visceral endoderm but not definitive endoderm, was used previously to evaluate convergent extension defects in *Zfp568*^{chato} mutants (Garcia-Garcia et al., 2008). We found that in late-lethality *Trim28*^{chatwo} embryos the definitive endoderm (*Ttr*-negative) failed to narrow (supplementary material Fig. S2E,G) to the same extent as *Zfp568*^{chato} embryos (Garcia-Garcia et al., 2008). Altogether, our analysis shows that the embryonic defects in late-lethality *Trim28*^{chatwo} embryos strongly resemble defects in *Zfp568* mutants (Fig. 1E,F) (Garcia-Garcia et al., 2008).

Analysis of molecular markers in extra-embryonic tissues also highlighted similarities in the extra-embryonic phenotypes of *Zfp568*^{chato} mutants and late-lethality *Trim28*^{chatwo} embryos, although some phenotypic differences were notable. Like *Zfp568*^{chato} embryos, the yolk sac of *Trim28*^{chatwo} mutants had numerous bubble-like protrusions (Fig. 1C,D, arrowheads). However, yolk sac blisters in late-lethality *Trim28*^{chatwo} embryos were found throughout the entire yolk sac, whereas they often clustered in a region proximal to the embryo in *Zfp568*^{chato} mutants (Fig. 1C-F) (Shibata and Garcia-Garcia, 2011). In *Zfp568*^{chato} embryos, defects in placental morphogenesis originate from the failure of the allantois to extend and contact the chorion, as well as from an expansion of the chorionic trophoderm and failure of the ectoplacental cavity to collapse (Shibata and Garcia-Garcia, 2011). Similar to *Zfp568*^{chato} mutants, we found that the ectoplacental cavity failed to close in some late-lethality *Trim28*^{chatwo} embryos (Fig. 1B,D; supplementary material Fig. S2B,D) and that the allantois was always underdeveloped (supplementary material Fig. S2B,D,F,H). However, late-lethality *Trim28*^{chatwo} never showed an expansion of the chorionic trophoderm similar to *Zfp568*^{chato} mutants, as illustrated by the lack of the enlarged smooth yolk sac area characteristic of *Zfp568*^{chato} embryos (Fig. 1E,F, bracket with asterisk) (Shibata and Garcia-Garcia, 2011). Instead, the yolk sac of *Trim28*^{chatwo} mutants was covered with blisters and had a constricted appearance (Fig. 1C,D, arrowheads). Inspection of sagittal sections showed that all late-lethality *Trim28*^{chatwo} mutants had a reduced exocoelomic cavity compared with wild-type littermates (supplementary material Fig. S2), a phenotype that is likely to have contributed to their distinct constricted and collapsed appearance compared with *Zfp568*^{chato} embryos (Shibata and Garcia-Garcia, 2011).

Taken together, results from our phenotypic characterization suggest that *Trim28* is required to control the same morphogenetic processes as *Zfp568* in embryonic tissues. However, the differences between the phenotype of late-lethality *Trim28*^{chatwo} and *Zfp568*^{chato} embryos in extra-embryonic tissues argue that *chatwo* disrupts morphogenetic processes in addition to those regulated by *Zfp568*.

Conditional inactivation of *Trim28* in embryonic-derived tissues causes *chatwo* phenotypes

Our previous analysis of tetraploid chimeras showed that *Zfp568* is required in embryonic-derived tissues to control morphogenesis of embryonic and extra-embryonic tissues (Shibata and Garcia-Garcia, 2011). If *Trim28* is required to mediate *Zfp568* function, we predicted that *Trim28* should be required in the same tissues as *Zfp568*. We therefore used a floxed conditional allele of *Trim28* (*Trim28^{L2/KO}*; Cammas et al., 2000; Weber et al., 2002) to conditionally inactivate *Trim28* in embryonic-derived tissues using the *Sox2Cre* transgene, which mediates recombination in all embryonic cell types, as well as extra-embryonic mesoderm, from early developmental stages (Hayashi et al., 2002).

We found that *Sox2Cre; Trim28^{L2/KO}* embryos escaped the early E5.5 lethality caused by complete loss of *Trim28* function, and arrested at ~E8.5. The embryonic phenotype of *Sox2Cre; Trim28^{L2/KO}* mutants strongly resembled that of *Zfp568^{chatwo}* and *Trim28^{chatwo}* embryos, including a short anterior-posterior axis, a wavy neural tube and failure to undergo gut closure (Fig. 3A-D). Consistent with a role of *Trim28* in convergent extension, analysis of *Foxf1* expression showed that *Sox2Cre; Trim28^{L2/KO}* embryos had a shorter and wider lateral plate mesoderm (Fig. 3A,B). *Sox2Cre; Trim28^{L2/KO}* embryos did not show the yolk sac protrusions or trophoblast malformations characteristic of *Trim28^{chatwo}* and *Zfp568^{chatwo}* mutants (Fig. 3B,D, arrowheads). However, similar to *Zfp568* mutant embryos (Shibata and Garcia-Garcia, 2011), yolk sac vasculogenesis was disrupted in *Sox2Cre; Trim28^{L2/KO}* mutants, as visualized by retention of embryonic blood cells in blood islands (not shown) and PECAM staining (Fig. 3E-H).

During early embryogenesis, *Trim28* is expressed in both embryonic and extra-embryonic tissues (supplementary material Fig. S3A) (Cammass et al., 2000). In situ hybridization experiments confirmed that *Trim28* expression was effectively reduced in embryonic-derived tissues of *Sox2Cre; Trim28^{L2/KO}* embryos (supplementary material Fig. S3A,B, solid arrowheads) and that, consistent with the lack of *Sox2Cre* expression in the trophoblast (Hayashi et al., 2002), *Trim28* expression was still expressed at high levels in this tissue (supplementary material Fig. S3A,B, open arrowheads). Western blotting indicated that although conditional inactivation of *Trim28* with *Sox2Cre* substantially reduced the levels of TRIM28, a small amount of protein could still be detected in embryonic tissues (supplementary material Fig. S3C). Thus, it is possible that either *Trim28* expression in the trophoblast or the small amount of TRIM28 protein in embryonic tissues could be responsible for the milder yolk sac phenotype of *Sox2Cre; Trim28^{L2/KO}* mutants compared with *Trim28^{chatwo}* embryos. Regardless, the resemblance of *Sox2Cre; Trim28^{L2/KO}* embryos to *Zfp568* and *Trim28^{chatwo}* mutants in embryonic tissues demonstrates further that TRIM28 is required for mammalian convergent extension.

TRIM28 forms transcriptional repressor complexes with ZFP568

The similarities between *Trim28^{chatwo}* and *Zfp568^{chatwo}* prompted us to examine whether TRIM28 interacts physically with ZFP568 and is required for ZFP568 transcriptional activity.

Yeast two-hybrid experiments showed that TRIM28 binds ZFP568 and that the interaction is mediated by the ZFP568 KRAB domain region (Fig. 4A). The interaction between TRIM28 and ZFP568 was also observed in mammalian cells, as revealed by co-immunoprecipitation experiments (Fig. 4B). TRIM28 has been

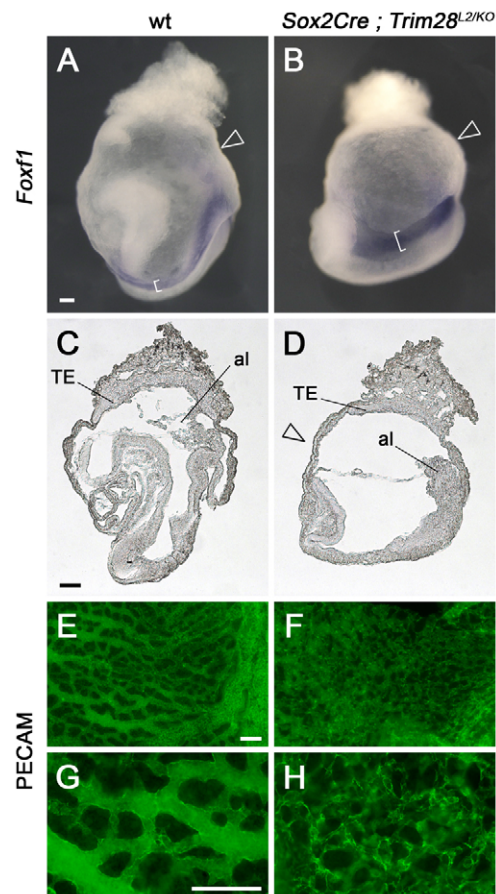


Fig. 3. *Trim28* is required in embryonic-derived cells. (A-H) Wild-type (A,C,E,G) and *Sox2Cre; Trim28^{L2/KO}* (B,D,F,H) E8.5 mouse embryos were analyzed by whole-mount in situ hybridization with a *Foxf1* probe (A,B) and in sagittal sections (C,D). Yolk sacs were stained with anti-PECAM antibodies to highlight the vascular plexus (E-H). Brackets in A and B highlight the lateral plate mesoderm. Arrowheads point to the yolk sac, which has a smooth appearance in *Sox2Cre; Trim28^{L2/KO}* embryos. TE, trophoblast; al, allantois. G and H are high magnifications of E and F, respectively. Scale bars: 100 μ m.

shown to be enriched at heterochromatic puncta in the nuclei of NIH3T3 cells (Nielsen et al., 1999). We found that GFP-tagged ZFP568 colocalized with TRIM28 in the nucleus of NIH3T3 cells and was present in the same heterochromatic foci (Fig. 4C). Taken together, these results show that TRIM28 and ZFP568 form protein complexes in the nucleus, consistent with a role in regulation of gene expression.

To determine whether TRIM28 mediates ZFP568 transcriptional activity, we used mammalian luciferase reporter assays. We found that a GAL4DBD-ZFP568 chimeric protein efficiently repressed expression of a 5xUAS-luciferase reporter in HEK293 cells (Fig. 5A, lane 1). This repression was enhanced in a dose-dependent fashion when increasing amounts of MYC-TRIM28 were transfected (Fig. 5A, lanes 2-4). Conversely, the ability of GAL4DBD-ZFP568 to repress transcription (Fig. 5B, lanes 1,2) was reduced when endogenous levels of TRIM28 were decreased using TRIM28 siRNAs (Fig. 5B, lanes 3,4). These experiments demonstrate that ZFP568 functions as a transcriptional repressor in vitro and that its ability to repress in these luciferase assays is dependent on the level of TRIM28.

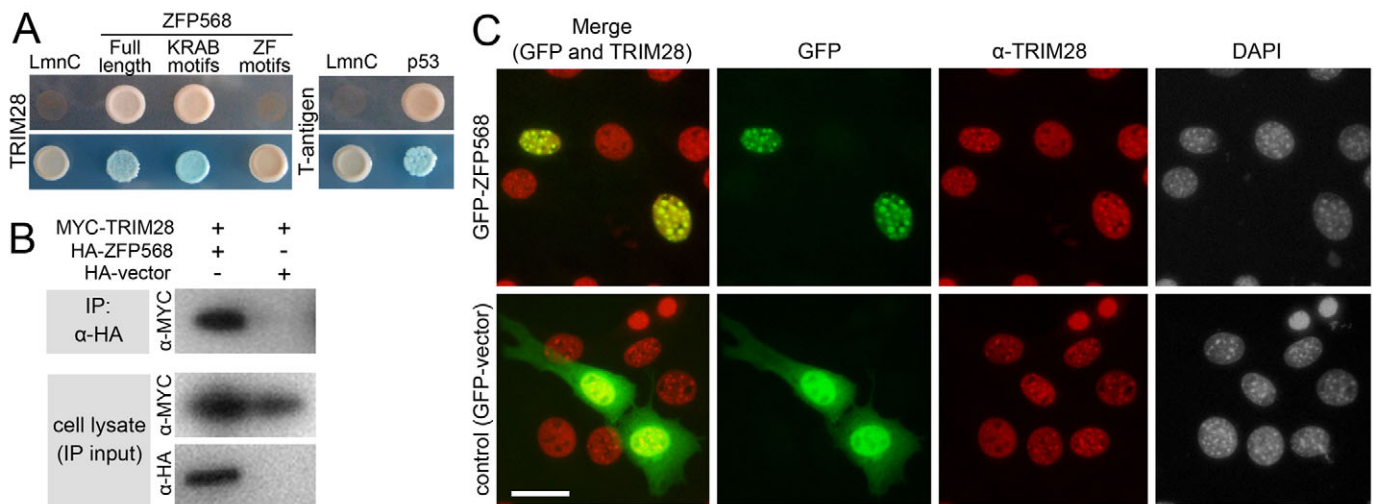


Fig. 4. ZFP568 interacts with TRIM28. (A) Yeast two-hybrid assays showed interaction of GAL4DBD-ZFP568 (full length and KRAB domains constructs) with GAL4AD-TRIM28, as indicated by growth in Ade-His-Leu-Trp-media (top panel) and blue colony color in Leu-Trp- X-alpha-gal plates (lower panel). GAL4DBD-ZFP568 zinc finger region did not interact with GAL4AD-TRIM28. Lamin C (LmnC) was used as a negative control. p53 interaction with SV40 large T-antigen was used as a positive control. (B) HA-ZFP568 and MYC-TRIM28 co-immunoprecipitate (IP) when transfected in HEK293 cells. (C) Subcellular localization of TRIM28 (red) and GFP-ZFP568 (top row, green) in NIH3T3 cells. An empty GFP vector was used as control (bottom panels, green). Samples were co-stained with DAPI. Scale bar: 50 μ m.

chatwo mutations affect the protein stability and repressive activity of TRIM28

To determine the molecular basis for the effects of the hypomorphic *chatwo* mutation on TRIM28, we first tested the ability of TRIM28^{chatwo} to provide ZFP568-mediated transcriptional repression in luciferase assays similar to those shown in Fig. 5. We found that GAL4DBD-ZFP568 repression increased in the presence of increasing amounts of FLAG-TRIM28^{chatwo} (Fig. 6A; compare red and gray luciferase levels), indicating that TRIM28^{chatwo} could bind to the KRAB domain of ZFP568 and mediate transcriptional repression. In agreement with this result, we found that TRIM28^{chatwo} was still able to interact with ZFP568 in yeast two-hybrid assays (supplementary material Fig. S4A). GAL4DBD-ZFP568 transcriptional repression in the presence of ectopic FLAG-TRIM28^{chatwo} was slightly reduced compared with when similar amounts of wild-type FLAG-TRIM28 were transfected (Fig. 6A, compare blue and red bars), but was not as severely affected compared with similar experiments using a sumoylation-deficient FLAG-TRIM28^{6KR} previously described to impair TRIM28 repressive activity (Masclé et al., 2007) (Fig. 6A, compare red and green bars). These results indicate that *chatwo* mutations decrease, but do not completely disrupt, TRIM28-mediated ZFP568 transcriptional repression activity.

It is noteworthy that the amount of FLAG-TRIM28^{chatwo} protein in cells was lower than in cells transfected with an equal amount of wild-type FLAG-TRIM28 (Fig. 6A, anti-FLAG western lanes 2-7). This result was not an artifact of the tagged forms of TRIM28 used in these experiments, as we obtained similar results with different FLAG- and MYC-tagged versions of TRIM28^{chatwo} (Fig. 6; data not shown). Moreover, the reduced protein levels produced by TRIM28^{chatwo} transgenes appeared to be specific to the *chatwo* mutations, as the sumoylation-deficient FLAG-TRIM28^{6KR} was expressed at similar levels to wild-type FLAG-TRIM28 (Fig. 6A, compare anti-FLAG western blot lanes 2-4 with lanes 8-10). Plasmids encoding FLAG-TRIM28 and FLAG-TRIM28^{chatwo} produced similar protein levels in a reticulocyte translation system

(supplementary material Fig. S5A), indicating that *chatwo* mutations do not affect the translation efficiency of these plasmids. Therefore, our results suggest that *chatwo* mutations affect the protein stability and/or rate of degradation of TRIM28.

We found that transfection of FLAG-TRIM28^{chatwo} decreased the levels of GAL4DBD-ZFP568 protein in cells (Fig. 6A, anti-Gal4DBD western blot compare lanes 2-7 with lane 1), as well as protein levels from transgenes containing other KRAB domain proteins, including ZFP57 and ZFP809 (not shown). Because TRIM28^{chatwo} was still able to interact with ZFP568 in yeast two-hybrid assays (supplementary material Fig. S4A), our results suggest that *chatwo* mutations affect the stability of TRIM28-KRAB domain proteins complexes, a hypothesis consistent with previous reports indicating that the stability of KRAB domain proteins depends on TRIM28 (Peng et al., 2000; Wolf and Goff, 2009).

Because the effects of *chatwo* mutations on the stability of TRIM28 and TRIM28-KRAB protein complexes could be responsible for the reduced transcriptional repression activity of FLAG-TRIM28^{chatwo} in GAL4DBD-ZFP568 luciferase assays (Fig. 6A), we investigated further whether *chatwo* mutations disrupt the transcriptional repressor activity of TRIM28. For this, we tested the ability of wild-type, *chatwo* mutant and sumoylation-deficient versions of a GAL4DBD-TRIM28 chimeric protein to repress directly expression of the 5xUAS-luciferase reporter (Fig. 6B). As previously shown (Masclé et al., 2007), GAL4DBD-TRIM28 repressed luciferase reporter expression in a dose-dependent fashion (Fig. 6B, blue) and the sumoylation-deficient GAL4DBD-TRIM28^{6KR} was not able to repress as efficiently (Fig. 6B, green). Similar to the effect of *chatwo* mutations on TRIM28 stability observed previously (Fig. 6A), cells transfected with GAL4DBD-TRIM28^{chatwo} contained lower levels of the chimeric protein than cells transfected with the same amount of wild-type GAL4DBD-TRIM28 (Fig. 6B, compare anti-GAL4DBD western blots). However, the ability of GAL4DBD-TRIM28^{chatwo} to repress transcription was reduced compared with similar levels of wild-type GAL4DBD-TRIM28 protein (Fig. 6B, compare 800 ng

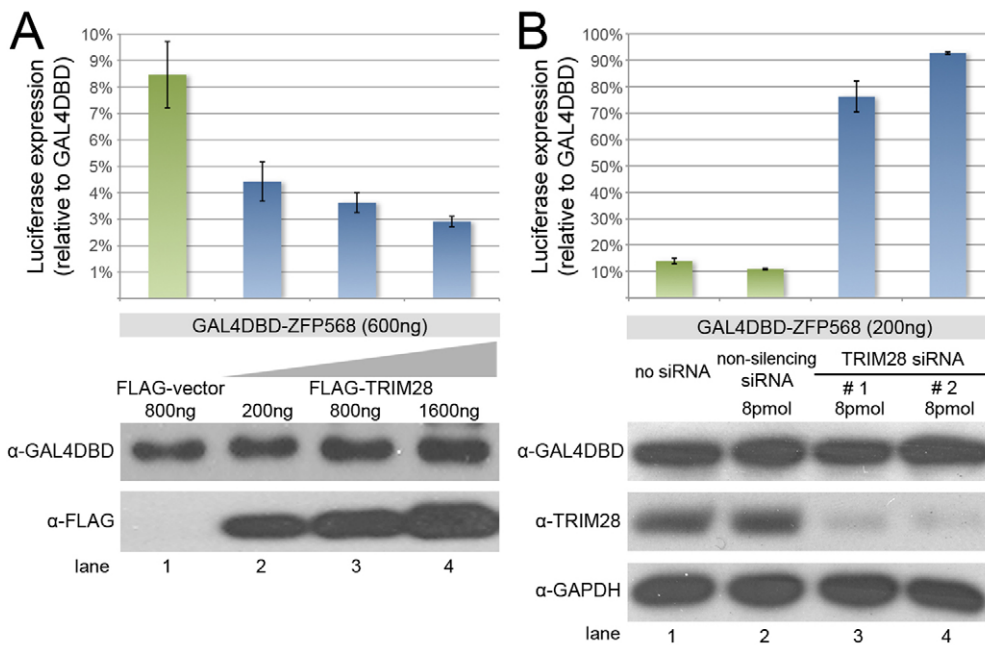


Fig. 5. TRIM28 mediates ZFP568 repressive activity. Quantification of luciferase expression from a 5xUAS-luciferase reporter in HEK293T cells, in the presence of GAL4DBD-ZFP568 and (A) absence (green)/presence (blue) of increasing amounts of FLAG-TRIM28 or (B) treatment with *Trim28* siRNAs (blue). Luciferase expression is plotted as the percentage relative to Gal4DBD empty vector (100%). Error bars represent s.d. Western blots show levels of ZFP568-Gal4DBD and FLAG-TRIM28 protein normalized for transfection efficiency. GAPDH serves as loading control for the siRNAs, which were introduced through an independent transfection event (see Materials and methods). Results in B represent one of six experiments showing similar results.

GAL4DBD-TRIM28^{chatwo} in lane 5 with 200 ng GAL4DBD-TRIM28 in lane 3), but was not as impaired as that of GAL4DBD-TRIM28^{GKR}. The ability of TRIM28^{chatwo} to repress transcription in the context of our cell transfection experiments is consistent with results from co-immunoprecipitation experiments showing that MYC-tagged TRIM28^{chatwo} could still recruit the chromatin-modifiers SETDB1 and CHD3 (supplementary material Fig. S4B). Altogether, these assays demonstrate that, independent of their effect on TRIM28 protein levels, *chatwo* mutations impair, but do not completely eradicate, TRIM28 repressive activity.

Repression of TRIM28 targets is disrupted in *chatwo* mutant embryos

To determine whether results from the molecular characterization of TRIM28's *chatwo* mutations held true in vivo, we sought to determine whether the protein levels and transcriptional repressive activity of TRIM28 were disrupted in *chatwo* mutant embryos. Western blotting determined that E7.5 *chatwo* mutants contained ~40-55% the level of TRIM28 protein present in wild-type littermate embryos (Fig. 7A; supplementary material Fig. S6), but transcript levels were normal, as tested by qRT-PCR (Fig. 7B). Therefore, this result confirms our previous findings and provides evidence that *chatwo* mutations affect the stability and/or rate of degradation of TRIM28 during early mouse development.

TRIM28 has been reported to repress expression of retrotransposons, including IAPs (Rowe et al., 2010). Therefore, we quantified the levels of IAP expression as a readout of TRIM28^{chatwo} repressive activity. qRT-PCR showed that IAP elements were expressed at high levels in *chatwo* mutant embryos compared with wild-type littermate controls (26±3.45 fold; Fig. 7C, light gray). However, the levels of IAP expression in *Trim28*^{chatwo} mutants were not as pronounced as in *Trim28*^{KO} embryos (87.26±18.34 fold; Fig. 7C, dark gray). These experiments demonstrate that *chatwo* mutations disrupt, but do not completely eliminate the repressive activity of TRIM28 in vivo. Because IAP silencing was not disrupted in *Zfp568*^{chato} mutants, these results further corroborate that *chatwo* mutations affect ZFP568-independent functions of TRIM28 (Fig. 7C).

DISCUSSION ZFP568-TRIM28 complexes control convergent extension and morphogenesis of extra-embryonic tissues

On the basis of its ability to bind KRAB domains and mediate transcriptional repression, TRIM28 has been proposed to be the universal co-repressor of all KRAB domain proteins (Urrutia, 2003). However, the roles of TRIM28 as a universal KRAB co-repressor are poorly understood, partly owing to the lack of knowledge about the biological functions of individual KRAB domain proteins. The phenotypic similarities between *Trim28*^{chatwo} and *Zfp568*^{chato} mutants, together with the identification of *chatwo* as a hypomorphic allele of *Trim28*, provide strong genetic evidence that ZFP568 and TRIM28 control convergent extension and morphogenesis of extra-embryonic tissues through a common molecular mechanism. This conclusion is further supported by the phenotype of embryos with a conditional inactivation of *Trim28* in embryonic-derived tissues (*Sox2Cre*; *Trim28*^{L2/KO} embryos), which display defects similar to *Trim28*^{chatwo} and *Zfp568*^{chato} mutants in embryonic tissues (Fig. 3; supplementary material Table S2). We show that ZFP568 and TRIM28 interact physically and colocalize in heterochromatic foci, and demonstrate that TRIM28 is required to mediate ZFP568 transcriptional repression. These results demonstrate an essential role of TRIM28 as a co-factor of ZFP568, and are consistent with the notion that ZFP568-TRIM28 complexes control morphogenetic processes through transcriptional repression.

chatwo mutations disrupt TRIM28 protein stability and transcriptional repression activity

We have demonstrated genetically that *chatwo* is a hypomorphic allele of *Trim28*, and determined that *chatwo* mutations disrupt both TRIM28 protein stability and transcriptional activity in cell culture assays and in embryos.

Even though the effect of *chatwo* mutations on TRIM28 protein levels surely contributes to the phenotypes caused by this hypomorphic TRIM28 condition, mice with a 50% reduction in

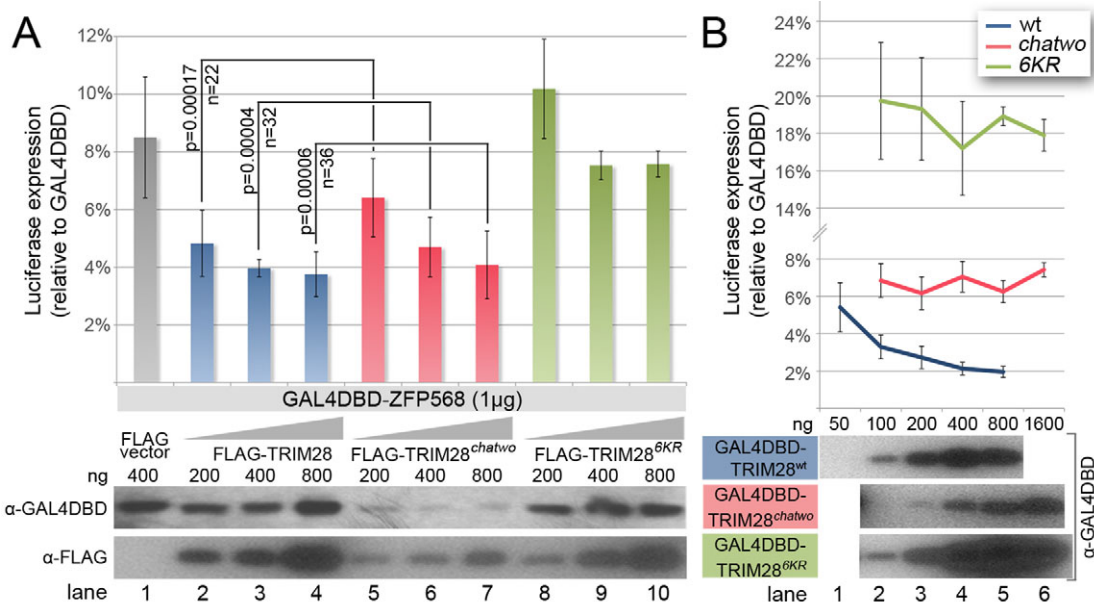


Fig. 6. *chatwo* mutations disrupt TRIM28 stability and repressive activity. Luciferase expression from a 5xUAS-luciferase reporter in HEK293T cells, (A) in the presence of GAL4DBD-ZFP568 and either FLAG empty vector (gray bar), increasing amounts of FLAG-TRIM28 (blue), Flag-TRIM28^{chatwo} (red) or Flag-TRIM28^{6KR} (green); (B) in the presence of GAL4DBD-TRIM28^{wt} (blue line), GAL4DBD-TRIM28^{chatwo} (red line) or GAL4DBD-TRIM28^{6KR} (green line). Note that the dose-dependent effect of GAL4DBD-TRIM28^{wt} (blue line) is lost in GAL4DBD-TRIM28^{chatwo} and GAL4DBD-TRIM28^{6KR} mutants (red and green lines, respectively). Luciferase expression is plotted as the percentage relative to GAL4DBD empty vector (100%). Error bars represent s.d. Results in A represent one of nine experiments showing similar results. P-values were calculated using data from all nine experiments (n =total number of data points). Western blots show levels of chimeric proteins normalized for transfection efficiency. Levels of GAL4DBD-ZFP568 in the presence of FLAG-TRIM28^{chatwo} were significantly lower compared with FLAG-vector conditions in six out of seven western blot experiments.

TRIM28 levels are viable (Whitelaw et al., 2010). Therefore, we find it unlikely that the 45-60% reduction in TRIM28 protein levels caused by *chatwo* mutations, alone, can explain the lethality and severity of morphological defects in *Trim28^{chatwo}* embryos. Instead, we favor the hypothesis that the phenotype of *Trim28^{chatwo}* mutants originates from the effects of *chatwo* mutations on both TRIM28 protein stability and transcriptional activity.

According to the available three dimensional structure of TRIM28's PHD-bromodomain region (Zeng et al., 2008), *chatwo* mutations are located in an area of the bromodomain facing the adjacent PHD motif. We hypothesize that *chatwo* mutations might disrupt either the folding of the bromodomain or its interaction with the adjacent PHD motif, a configuration that might be important for the ability of TRIM28 to form functional transcriptional repressor complexes. The PHD domain of TRIM28 has been shown to promote intramolecular sumoylation of the neighboring bromodomain, a modification that impacts TRIM28 transcriptional activity (Ivanov et al., 2007; Mascle et al., 2007). We find it unlikely that the effect of *chatwo* mutations on TRIM28 repressive activity is due to lack of sumoylation, as *chatwo* mutations do not affect any of TRIM28's sumoylated lysine residues, and the repressive activity of a sumoylation-deficient TRIM28 is far more reduced than that of TRIM28^{chatwo} (Fig. 6B, compare TRIM28^{chatwo}-red and TRIM28^{6KR}-green). Because TRIM28's C-terminal bromodomain has been involved in recruitment of chromatin-modifying enzymes, including SETDB1 and CHD3 (Schultz et al., 2002; Sripathy et al., 2006), we favor the hypothesis that *chatwo* mutations affect TRIM28 repressive activity by interfering with the recruitment of these factors or other possible transcriptional co-factors that are as yet unknown.

TRIM28 influences the stability of KRAB domain proteins

Consistent with previous reports (Peng et al., 2000; Wolf and Goff, 2009), the molecular characterization of *chatwo* presented here indicates that the levels of TRIM28 in cells impinge on the stability of ZFP568 and other KRAB domain proteins (Fig. 6). We found that the effects of TRIM28 on KRAB domain protein levels were dependent on the relative amount of each protein within the cell. Hence, increasing amounts of tagged-TRIM28 stabilized GAL4DBD-ZFP568 in a dose-dependent fashion only when the latter was transfected in excess (compare results in Fig. 6A with those of Fig. 5A). Notably, we did not observe destabilization of GAL4DBD-ZFP568 upon TRIM28 siRNA treatment (Fig. 5B), a surprising result given that stability of other KRAB domain proteins has been previously described to decrease upon TRIM28 knockdown (Wolf and Goff, 2009). We attribute this discrepancy to differences in the experimental design and/or in the affinity of distinct KRAB domain proteins for TRIM28 between our experiments and those previously published. Nevertheless, our cell culture experiments showed a consistent effect of *chatwo* mutations in destabilizing transfected GAL4DBD-ZFP568 (Fig. 6A, lanes 5-7).

Although an effect of *Trim28^{chatwo}* mutations on ZFP568 protein stability could lead to a dominant loss-of-function effect in embryos, we have not observed any genetic evidence suggesting a possible antimorphic activity of the *chatwo* allele. Namely, we did not observe any dominant phenotype associated with *chatwo* heterozygote animals, nor did we observe a genetic interaction between *Trim28^{chatwo}* and *Zfp568^{chato}* in double heterozygote embryos (supplementary material Fig. S8). Therefore, further

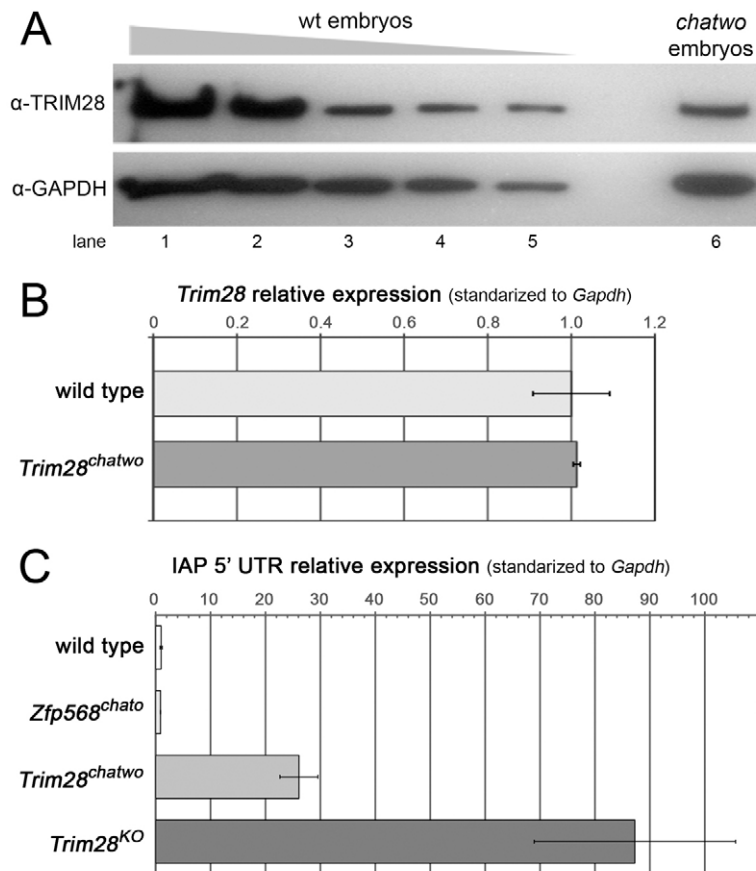


Fig. 7. *chatwo* mutations disrupt TRIM28 stability and repressive activity in vivo. (A) Western blot using an anti-TRIM28 antibody and lysates from a gradient of decreasing amounts of E7.5 wild-type extract (lanes 1-5) and a pool of six *chatwo* mouse embryos (lane 6). Lanes 1 to 5 represent lysates from approximately 4, 2, 1, 0.5 and 0.25 wild-type embryos, respectively. Anti-GAPDH antibody was used as a loading control (lower panel). The TRIM28 antibody was raised against part of the coiled-coil and HP1-binding domain and was still able to recognize the *chatwo* mutant protein. Similar results were obtained using an anti-TRIM28 polyclonal antibody (data not shown). Quantification of TRIM28 levels is shown in supplementary material Fig. S6. Note that mRNA and protein levels of *Trim28* were unaffected in *Zfp568^{chato}* mutants and that *Zfp568* expression was normal in *Trim28^{chatwo}* embryos (supplementary material Fig. S7). (B) qRT-PCR analysis of *Trim28* expression in wild-type and *Trim28^{chatwo}* embryos. (C) Expression of IAP elements quantified by qRT-PCR in wild-type, *Zfp568^{chato}*, *Trim28^{chatwo}* and *Trim28^{KO}* embryos. qRT-PCR results show expression relative to the wild-type sample and normalized with respect to expression of *Gapdh*. Error bars represent s.d. between independent pools of embryos.

experiments using antibodies against ZFP568 and other specific KRAB domain proteins will be required to address whether the levels of TRIM28 within cells might be important to stabilize KRAB domain proteins in vivo.

***chatwo* mutations disrupt ZFP568-independent functions of TRIM28**

Whereas the phenotypic similarities between *Trim28^{chatwo}* and *Zfp568^{chato}* mutants in embryonic tissues revealed a functional link between ZFP568 and TRIM28, the differences between the extra-embryonic phenotypes of *Trim28^{chatwo}* and *Zfp568^{chato}* embryos (Fig. 1; supplementary material Table S2) uncovered ZFP568-independent roles of TRIM28 in the development of the yolk sac and placenta. This is consistent with results from the double mutant analysis between *Trim28^{chatwo}* and *Zfp568^{chato}* mutants (supplementary material Fig. S8), which showed that embryos simultaneously mutant for *Trim28^{chatwo}* and *Zfp568^{chato}* have extra-embryonic defects more similar to those of *Trim28^{chatwo}* embryos. Additionally, we have obtained evidence indicating that *chatwo* mutations affect ZFP568-independent functions of TRIM28 that relate to silencing of retroviral elements and gastrulation processes required for embryo survival past E7.5. We speculate that these ZFP568-independent roles of TRIM28 could be carried out through its ability to interact with other KRAB domain proteins or additional proteins that might determine its transcriptional activity and/or targets.

TRIM28 is differentially required during early mouse embryogenesis

Embryos homozygous for the *Trim28^{chatwo}* hypomorph condition survive longer than *Trim28^{KO}* mice, which fail to gastrulate and which die at E5.5 (Cammass et al., 2000). This observation implies

that the reduced TRIM28 protein levels and repressive activity caused by *chatwo* mutations are sufficient to bypass TRIM28 requirements in pre-gastrula stage embryos, but not enough to fulfill the functions of TRIM28 past E7.5. Therefore, the identification and characterization of *Trim28^{chatwo}* embryos revealed that TRIM28 has separate requirements during the early stages of mouse development. Analysis of *Sox2Cre; Trim28^{L2/KO}* embryos also shed light on TRIM28 spatial and temporal requirements at early embryonic stages. The late lethality of *Sox2Cre; Trim28^{L2/KO}* embryos indicates that TRIM28 might be required in embryonic tissues at early developmental stages prior to *Sox2Cre* activity (Hayashi et al., 2002). Alternatively, it is possible that *Trim28* is required during pre-gastrula stages in the trophectoderm, a tissue that expresses high levels of *Trim28* and is not affected in *Sox2Cre; Trim28^{L2/KO}* embryos (supplementary material Fig. S3).

Because the DNA target specificity of TRIM28 is thought to depend on its interaction with other factors, mainly KRAB domain proteins (Urrutia, 2003), we hypothesize that the differences between phenotype and lethality of *Trim28* hypomorphic (*Trim28^{chatwo}*), conditional (*Sox2Cre; Trim28^{L2/KO}*) and null (*Trim28^{KO}*) conditions reflect that specific co-factors require different levels of TRIM28 activity.

Additionally, we obtained data indicating that TRIM28 requirements for a particular KRAB-domain protein might differ in a tissue-specific manner. Specifically, *Sox2Cre; Trim28^{L2/KO}* embryos showed similar embryonic morphogenetic defects to *Zfp568^{chato}* and late-arrest *Trim28^{chatwo}* embryos, but lacked the extra-embryonic malformations characteristic of these mutants. Therefore, it is possible that ZFP568 requires higher levels of TRIM28 to control morphogenesis of embryonic tissues than to

promote the development of the yolk sac and placenta. These differential requirements might be dictated by tissue-specific factors that could stabilize or modulate the activity of TRIM28 complexes with KRAB domain proteins or with other transcription factors.

In conclusion, the phenotypic and molecular characterization of the *Trim28^{chato}* hypomorphic allele described here provides strong genetic evidence that TRIM28 is required for ZFP568 function, identifies a novel role of *Trim28* in the control of mammalian convergent extension and reveals separate functions of *Trim28* during early mouse embryogenesis. Recent studies to identify TRIM28 genomic targets have challenged the role of KRAB domain proteins as determining factors for the biological functions of TRIM28 (Iyengar and Farnham, 2011; Iyengar et al., 2011). However, our findings demonstrate that the interaction of TRIM28 with ZFP568 is essential for embryonic morphogenesis and suggest that particular KRAB domain proteins dictate TRIM28 involvement in specific biological processes in vivo. Future studies to identify additional binding partners of TRIM28 and elucidate the specific roles of KRAB domain proteins will be required to understand the complexity of TRIM28 functions.

Acknowledgements

We thank Kathryn Anderson, Tim Bestor, Mathieu Boulard, Ken Kempthues, John Schimenti, members of the laboratory and anonymous reviewers for helpful discussions and comments on the manuscript; Drs Ruth Arkell, Muriel Aubry, Florence Cammas, James Cross, Vincent Giguère, Leif Lundh, Xavier Masclé, Ling Qi, Shao-Cong Sun and Ken-ichi Yamamura for mice and reagents; and Cornell's CARE staff for mice husbandry and care.

Funding

This work was supported by the National Institutes of Health [grant number R01HD060581 from the Eunice Kennedy Shriver National Institute of Child Health & Human Development to M.J.G.G., R01NS044385 to K.F.L.]; and by the National Science Foundation [IOS-1020878 to M.J.G.G.]. Deposited in PMC for release after 12 months.

Competing interests statement

The authors declare no competing financial interests.

Supplementary material

Supplementary material available online at <http://dev.biologists.org/lookup/suppl/doi:10.1242/dev.072546/-/DC1>

References

- Abrink, M., Ortiz, J. A., Mark, C., Sanchez, C., Looman, C., Hellman, L., Chambon, P. and Losson, R. (2001). Conserved interaction between distinct Kruppel-associated box domains and the transcriptional intermediary factor 1 beta. *Proc. Natl. Acad. Sci. USA* **98**, 1422-1426.
- Agata, Y., Matsuda, E. and Shimizu, A. (1999). Two novel Kruppel-associated box-containing zinc-finger proteins, KRAZ1 and KRAZ2, repress transcription through functional interaction with the corepressor KAP-1 (TIF1beta/KRIP-1). *J. Biol. Chem.* **274**, 16412-16422.
- Alter, M. D. and Hen, R. (2008). Putting a KAP on transcription and stress. *Neuron* **60**, 733-735.
- Anderson, K. V. (2000). Finding the genes that direct mammalian development: ENU mutagenesis in the mouse. *Trends Genet.* **16**, 99-102.
- Cammas, F., Mark, M., Dolle, P., Dierich, A., Chambon, P. and Losson, R. (2000). Mice lacking the transcriptional corepressor TIF1beta are defective in early postimplantation development. *Development* **127**, 2955-2963.
- Cammas, F., Oulad-Abdelghani, M., Vonesch, J. L., Huss-Garcia, Y., Chambon, P. and Losson, R. (2002). Cell differentiation induces TIF1beta association with centromeric heterochromatin via an HP1 interaction. *J. Cell Sci.* **115**, 3439-3448.
- Cammas, F., Herzog, M., Lerouge, T., Chambon, P. and Losson, R. (2004). Association of the transcriptional corepressor TIF1beta with heterochromatin protein 1 (HP1): an essential role for progression through differentiation. *Genes Dev.* **18**, 2147-2160.
- Candia, A. F., Hu, J., Crosby, J., Lalley, P. A., Noden, D., Nadeau, J. H. and Wright, C. V. (1992). Mox-1 and Mox-2 define a novel homeobox gene subfamily and are differentially expressed during early mesodermal patterning in mouse embryos. *Development* **116**, 1123-1136.
- Cereghini, S., Ott, M. O., Power, S. and Maury, M. (1992). Expression patterns of vHNF1 and HNF1 homeoproteins in early postimplantation embryos suggest distinct and sequential developmental roles. *Development* **116**, 783-797.
- Chang, C. J., Chen, Y. L. and Lee, S. C. (1998). Coactivator TIF1beta interacts with transcription factor C/EBPbeta and glucocorticoid receptor to induce alpha-1-acid glycoprotein gene expression. *Mol. Cell. Biol.* **18**, 5880-5887.
- Emerson, R. O. and Thomas, J. H. (2009). Adaptive evolution in zinc finger transcription factors. *PLoS Genet.* **5**, e1000325.
- Friedman, J. R., Fredericks, W. J., Jensen, D. E., Speicher, D. W., Huang, X. P., Neilson, E. G. and Rauscher, F. J., 3rd (1996). KAP-1, a novel corepressor for the highly conserved KRAB repression domain. *Genes Dev.* **10**, 2067-2078.
- Garcia-Garcia, M. J., Shibata, M. and Anderson, K. V. (2008). Chato, a KRAB zinc-finger protein, regulates convergent extension in the mouse embryo. *Development* **135**, 3053-3062.
- Gebelein, B. and Urrutia, R. (2001). Sequence-specific transcriptional repression by KS1, a multiple-zinc-finger-Kruppel-associated box protein. *Mol. Cell. Biol.* **21**, 928-939.
- Germain-Desprez, D., Bazinet, M., Bouvier, M. and Aubry, M. (2003). Oligomerization of transcriptional intermediary factor 1 regulators and interaction with ZNF74 nuclear matrix protein revealed by bioluminescence resonance energy transfer in living cells. *J. Biol. Chem.* **278**, 22367-22373.
- Hayashi, S., Lewis, P., Pevny, L. and McMahon, A. P. (2002). Efficient gene modulation in mouse epiblast using a Sox2Cre transgenic mouse strain. *Mech. Dev.* **119 Suppl.** **1**, S97-S101.
- Herzog, M., Wendling, O., Guillou, F., Chambon, P., Mark, M., Losson, R. and Cammas, F. (2010). TIF1beta association with HP1 is essential for post-gastrulation development, but not for Sertoli cell functions during spermatogenesis. *Dev. Biol.* **350**, 548-558.
- Ho, J., Kong, J. W., Choong, L. Y., Loh, M. C., Toy, W., Chong, P. K., Wong, C. H., Wong, C. Y., Shah, N. and Lim, Y. P. (2009). Novel breast cancer metastasis-associated proteins. *J. Proteome Res.* **8**, 583-594.
- Hu, G., Kim, J., Xu, Q., Leng, Y., Orkin, S. H. and Elledge, S. J. (2009). A genome-wide RNAi screen identifies a new transcriptional module required for self-renewal. *Genes Dev.* **23**, 837-848.
- Huntley, S., Baggott, D. M., Hamilton, A. T., Tran-Gyamfi, M., Yang, S., Kim, J., Gordon, L., Branscomb, E. and Stubbs, L. (2006). A comprehensive catalog of human KRAB-associated zinc finger genes: insights into the evolutionary history of a large family of transcriptional repressors. *Genome Res.* **16**, 669-677.
- Ivanov, A. V., Peng, H., Yurchenko, V., Yap, K. L., Negorev, D. G., Schultz, D. C., Pulkowski, E., Fredericks, W. J., White, D. E., Maul, G. G. et al. (2007). PHD domain-mediated E3 ligase activity directs intramolecular sumoylation of an adjacent bromodomain required for gene silencing. *Mol. Cell* **28**, 823-837.
- Iyengar, S. and Farnham, P. J. (2011). KAP1: an enigmatic master regulator of the genome. *J. Biol. Chem.* **286**, 26267-26276.
- Iyengar, S., Ivanov, A. V., Jin, V. X., Rauscher, F. J., 3rd and Farnham, P. J. (2011). Functional analysis of KAP1 genomic recruitment. *Mol. Cell. Biol.* **31**, 1833-1847.
- Jakobsson, J., Cordero, M. I., Bisaz, R., Groner, A. C., Buskamp, V., Bensadoun, J. C., Cammas, F., Losson, R., Mansuy, I. M., Sandi, C. et al. (2008). KAP1-mediated epigenetic repression in the forebrain modulates behavioral vulnerability to stress. *Neuron* **60**, 818-831.
- Kim, S. S., Chen, Y. M., O'Leary, E., Witzgall, R., Vidal, M. and Bonventre, J. V. (1996). A novel member of the RING finger family, KRIP-1, associates with the KRAB-A transcriptional repressor domain of zinc finger proteins. *Proc. Natl. Acad. Sci. USA* **93**, 15299-15304.
- Krebs, C. J., Larkins, L. K., Price, R., Tullis, K. M., Miller, R. D. and Robins, D. M. (2003). Regulator of sex-limitation (Rsl) encodes a pair of KRAB zinc-finger genes that control sexually dimorphic liver gene expression. *Genes Dev.* **17**, 2664-2674.
- Li, X., Ito, M., Zhou, F., Youngson, N., Zuo, X., Leder, P. and Ferguson-Smith, A. C. (2008). A maternal-zygotic effect gene, *Zfp57*, maintains both maternal and paternal imprints. *Dev. Cell* **15**, 547-557.
- Liem, K. F., Jr, He, M., Ocbina, P. J. and Anderson, K. V. (2009). Mouse *Kif7/Coastal2* is a cilia-associated protein that regulates Sonic hedgehog signaling. *Proc. Natl. Acad. Sci. USA* **106**, 13377-13382.
- Mahlpuu, M., Ormestad, M., Enerback, S. and Carlsson, P. (2001). The forkhead transcription factor *Foxf1* is required for differentiation of extra-embryonic and lateral plate mesoderm. *Development* **128**, 155-166.
- Masclé, X. H., Germain-Desprez, D., Huynh, P., Estephan, P. and Aubry, M. (2007). Sumoylation of the transcriptional intermediary factor 1beta (TIF1beta), the co-repressor of the KRAB Multifinger proteins, is required for its transcriptional activity and is modulated by the KRAB domain. *J. Biol. Chem.* **282**, 10190-10202.
- Moosmann, P., Georgiev, O., Le Douarin, B., Bourquin, J. P. and Schaffner, W. (1996). Transcriptional repression by RING finger protein TIF1 beta that interacts with the KRAB repressor domain of KOX1. *Nucleic Acids Res.* **24**, 4859-4867.
- Moran, J. L., Bolton, A. D., Tran, P. V., Brown, A., Dwyer, N. D., Manning, D. K., Bjork, B. C., Li, C., Montgomery, K., Siepka, S. M. et al. (2006).

- Utilization of a whole genome SNP panel for efficient genetic mapping in the mouse. *Genome Res.* **16**, 436-440.
- Nagy, A.** (2003). *Manipulating the Mouse Embryo: A Laboratory Manual*. Cold Spring Harbor, NY: Cold Spring Harbor Laboratory Press.
- Nielsen, A. L., Ortiz, J. A., You, J., Oulad-Abdelghani, M., Khechumian, R., Gansmuller, A., Chambon, P. and Losson, R.** (1999). Interaction with members of the heterochromatin protein 1 (HP1) family and histone deacetylation are differentially involved in transcriptional silencing by members of the TIF1 family. *EMBO J.* **18**, 6385-6395.
- Peng, H., Begg, G. E., Harper, S. L., Friedman, J. R., Speicher, D. W. and Rauscher, F. J.** (2000). Biochemical analysis of the Kruppel-associated box (KRAB) transcriptional repression domain. *J. Biol. Chem.* **275**, 18000-18010.
- Peng, H., Feldman, I. and Rauscher, F. J., 3rd** (2002). Hetero-oligomerization among the TIF family of RBCC/TRIM domain-containing nuclear cofactors: a potential mechanism for regulating the switch between coactivation and corepression. *J. Mol. Biol.* **320**, 629-644.
- Quertermous, E. E., Hidai, H., Blonar, M. A. and Quertermous, T.** (1994). Cloning and characterization of a basic helix-loop-helix protein expressed in early mesoderm and the developing somites. *Proc. Natl. Acad. Sci. USA* **91**, 7066-7070.
- Rambaud, J., Desroches, J., Balsalobre, A. and Drouin, J.** (2009). TIF1beta/KAP-1 is a coactivator of the orphan nuclear receptor NGFI-B/Nur77. *J. Biol. Chem.* **284**, 14147-14156.
- Rowe, H. M., Jakobsson, J., Mesnard, D., Rougemont, J., Reynard, S., Aktas, T., Maillard, P. V., Layard-Liesching, H., Verp, S., Marquis, J. et al.** (2010). KAP1 controls endogenous retroviruses in embryonic stem cells. *Nature* **463**, 237-240.
- Ryan, R. F., Schultz, D. C., Ayyanathan, K., Singh, P. B., Friedman, J. R., Fredericks, W. J. and Rauscher, F. J.** (1999). KAP-1 corepressor protein interacts and colocalizes with heterochromatic and euchromatic HP1 proteins: a potential role for Kruppel-associated box-zinc finger proteins in heterochromatin-mediated gene silencing. *Mol. Cell. Biol.* **19**, 4366-4378.
- Schultz, D. C., Friedman, J. R. and Rauscher, F. J., 3rd** (2001). Targeting histone deacetylase complexes via KRAB-zinc finger proteins: the PHD and bromodomains of KAP-1 form a cooperative unit that recruits a novel isoform of the Mi-2alpha subunit of NuRD. *Genes Dev.* **15**, 428-443.
- Schultz, D. C., Ayyanathan, K., Negorev, D., Maul, G. G. and Rauscher, F. J., 3rd** (2002). SETDB1: a novel KAP-1-associated histone H3, lysine 9-specific methyltransferase that contributes to HP1-mediated silencing of euchromatic genes by KRAB zinc-finger proteins. *Genes Dev.* **16**, 919-932.
- Seki, Y., Kurisaki, A., Watanabe-Susaki, K., Nakajima, Y., Nakanishi, M., Arai, Y., Shiota, K., Sugino, H. and Asashima, M.** (2010). TIF1beta regulates the pluripotency of embryonic stem cells in a phosphorylation-dependent manner. *Proc. Natl. Acad. Sci. USA* **107**, 10926-10931.
- Shibata, M. and Garcia-Garcia, M. J.** (2011). The mouse KRAB zinc-finger protein CHATO is required in embryonic-derived tissues to control yolk sac and placenta morphogenesis. *Dev. Biol.* **349**, 331-341.
- Shin, J. H., Ko, H. S., Kang, H., Lee, Y., Lee, Y. I., Pletinkova, O., Troconso, J. C., Dawson, V. L. and Dawson, T. M.** (2011). PARIS (ZNF746) repression of PGC-1alpha contributes to neurodegeneration in Parkinson's disease. *Cell* **144**, 689-702.
- Sripathy, S. P., Stevens, J. and Schultz, D. C.** (2006). The KAP1 corepressor functions to coordinate the assembly of de novo HP1-demarcated microenvironments of heterochromatin required for KRAB zinc finger protein-mediated transcriptional repression. *Mol. Cell. Biol.* **26**, 8623-8638.
- Urrutia, R.** (2003). KRAB-containing zinc-finger repressor proteins. *Genome Biol.* **4**, 231.
- Weber, P., Cammas, F., Gerard, C., Metzger, D., Chambon, P., Losson, R. and Mark, M.** (2002). Germ cell expression of the transcriptional co-repressor TIF1beta is required for the maintenance of spermatogenesis in the mouse. *Development* **129**, 2329-2337.
- Whitelaw, N. C., Chong, S., Morgan, D. K., Nestor, C., Bruxner, T. J., Ashe, A., Lambley, E., Meehan, R. and Whitelaw, E.** (2010). Reduced levels of two modifiers of epigenetic gene silencing, Dnmt3a and Trim28, cause increased phenotypic noise. *Genome Biol.* **11**, R111.
- Wilkinson, D. G., Bhatt, S. and Herrmann, B. G.** (1990). Expression pattern of the mouse T gene and its role in mesoderm formation. *Nature* **343**, 657-659.
- Wolf, D. and Goff, S. P.** (2007). TRIM28 mediates primer binding site-targeted silencing of murine leukemia virus in embryonic cells. *Cell* **131**, 46-57.
- Wolf, D. and Goff, S. P.** (2009). Embryonic stem cells use ZFP809 to silence retroviral DNAs. *Nature* **458**, 1201-1204.
- Wolf, D., Cammas, F., Losson, R. and Goff, S. P.** (2008a). Primer binding site-dependent restriction of murine leukemia virus requires HP1 binding by TRIM28. *J. Virol.* **82**, 4675-4679.
- Wolf, D., Hug, K. and Goff, S. P.** (2008b). TRIM28 mediates primer binding site-targeted silencing of Lys1,2 tRNA-utilizing retroviruses in embryonic cells. *Proc. Natl. Acad. Sci. USA* **105**, 12521-12526.
- Yokoe, T., Toyama, Y., Okugawa, Y., Tanaka, K., Ohi, M., Inoue, Y., Mohri, Y., Miki, C. and Kusunoki, M.** (2009). KAP1 is associated with peritoneal carcinomatosis in gastric cancer. *Ann. Surg. Oncol.* **17**, 821-828.
- Zeng, L., Yap, K. L., Ivanov, A. V., Wang, X., Mujtaba, S., Plotnikova, O., Rauscher, F. J., 3rd and Zhou, M. M.** (2008). Structural insights into human KAP1 PHD finger-bromodomain and its role in gene silencing. *Nat. Struct. Mol. Biol.* **15**, 626-633.